# The first principle calculations of structural, magneto-electronic, elastic, mechanical, and thermoelectric properties of half-metallic double perovskite oxide $Sr_2TiCoO_6$

L. F. Blaha[a], A. Maafa[a], H. Rozale[a,*], A. Chahed[a], M.A.H. Boukli[a] and A. Sayade[b]

[a] *Condensed Matter and sustainable development Laboratory (LMCDD), University of Sidi Bel-Abbes, Sidi Bel-Abbes 22000, Algeria.*
**e-mail: hrozale@yahoo.fr; hrozale@univ-sba.dz*
[b] *Univ. Artois, CNRS, Centrale Lille, ENSCL, Univ. Lille, UMR 8181-UCCS-Unité de Catalyse et Chimie du Solide, F-59000 Lille, France*

Received 23 July 2020; accepted 20 October 2020

The structural, elastic, mechanical, magneto-electronic, and thermoelectric properties of $Sr_2TiCoO_6$ double perovskite oxide have been studied within the framework of density functional theory. The FP-LAPW method within the (GGA) and (mBJ) approximations is chosen in the computational approach. This alloy crystallizes in a cubic structure with the ferromagnetic phase. The computed lattice constant was found to agree with the available experimental results. This compound shows the half-metallic ferromagnetic properties. A value of 1 $\mu$B is found for the total magnetic moment with an important contribution from Co atoms. The elastic parameters reveal that Sr2TiCoO6 as being super hard and brittle. We calculated the thermoelectric properties of $Sr_2TiCoO_6$ using the Boltzmann transport equations within the DFT in a temperature range from 100 to 1000 K. The transport parameters like Seebeck coefficient, electrical thermal conductivity, the electrical conductivity, and the power factor, have been put together to establish their thermoelectric response. Our findings clearly demonstrate an improvement in the power factor with increasing temperature.

*Keywords:* Density functional theory; double perovskite oxide; half-metallic; ferromagnetic; elastic and mechanical properties; transport properties.

PACS: 31.15.E-; 72.25-b; 75.30.C; 75.50.Dd; 87.19.rd; 51.35.+a; 52.25.Fi

DOI: https://doi.org/10.31349/RevMexFis.67.114

## 1. Introduction

The large energy consumption, contamination, and decreased energy sources are a major problem for the world energy crisis [1]. Similarly, the harmful emissions caused by fossil fuels also present a serious threat to our ecological balance. In order to resolve these issues, scientists are seeking newly affordable, effective, and environmentally friendly alternatives to energy resources like wind biofuels, photovoltaics, and thermoelectric energy conversion devices [2]. Thermoelectric devices based on the Seebeck effect are responsible for transforming waste heat into usable electrical energy thus minimizing energy waste. These devices are consequently proving to be relatively economical and are a source of renewable energy [3-6].

Materials such as perovskites have gained a great deal of attention due to their multifunctional character [7] and have therefore been a major subject of interest. Perovskites with $ABO_3$ structure have been extensively studied for their physical and chemical properties [8-11], by either doping or simply duplicating the lattice sizes resulting in the creation of a double perovskite. Such systems can be more efficient when filling the cation's site. Double perovskites are a very recent class of materials with a general $A_2BB'O_6$ formula where A site is occupied by a rare-earth or alkaline-earth metal, B and B'sites are occupied by different cations (transition/non-transition metals) depending on their charge and the ion size [12].

Due to their remarkable properties such as half-metallicity, ferromagnetism, and high thermopower, the transition-metal-based double perovskites have received considerable attention in various technologically important fields, applied and fundamental areas of material science [13,14]. Another significant factor in the application of organic-inorganic hybrid perovskites in solar thermoelectric generators is the conversion of sunlight to electricity [14,15].

Acharya *et al*. [16] have evaluated $Sr_2TiCoO_6$ based double perovskites modified by aliovalent substitution of $Bi^{+3}$ in Sr-site for high-temperature thermoelectric applications. Further, Saxena *et al*. [17] have reported the synthesis and thermoelectric properties of $Sr_2TiCoO_6$ and $Sr_2TiMoO_6$ double perovskites experimentally. They have also confirmed the cubic structure with $Fm\bar{3}m$ (225) space group in these ceramics with a lattice constant of 7.35 A°. Sudha *et al*. have investigated the effect of calcium doping on the structure and thermoelectric properties of $Sr_2TiCoO_6$ (STC) double perovskites. It has been found to possess a cubic crystal structure with a $Pm\bar{3}m$ space group as confirmed by Rietveld refinement of XRD data with a lattice constant of about 3.896 A° [18].

Nevertheless, to the best of our knowledge, no detailed studies on the recently synthesized Cubic $Sr_2TiCoO_6$ double

perovskites have been investigated in the literature using ab-initio calculations.

This research was carried out to investigate the structural, magneto-electronic, and elastic properties of $Sr_2TiCoO_6$ in its cubic structure from the first principles of DFT calculations, which are followed by the transport properties using semi-classical Boltzmann theory.

## 2. Computational details

The first principles-based spin-polarized full potential linearly augmented plane wave method (SP-FPLAPW) [19] as implemented in the Wien2k code [20] has been used to calculate highly precise ground state properties of the present material. Two different approximation methods, generalized gradient approximation (GGA) [21] and modified Becke-Johnson (mBJ) [22] were employed for the exchange-correlation potential. The basis set inside each muffin-tin sphere is split into core and valence states. The core states are treated within the spherical part of the potential and are assigned to have spherically symmetric charge density confined within the muffin-tin spheres. The cut-off parameter $RMT$ $K$max in the basis set is chosen to be 7 [23] where $K$Max is the plane wave cut-off and RMT is the smallest muffin-tin radius. The cut-off energy, which defines the separation among the core and the valence states, was set at -8.0 Ry.

400 k-points are used in the calculations. The total charge and energy convergence are taken to be $10^{-4}$ Ry and $10^{-4}$ a.u$^3$ respectively. Elastic constants calculations have been done within the scheme developed by Charpin [24] as integrated into WIEN2K. The transport properties are calculated within the framework of semiclassical Boltzmann theory by using the BoltzTraP code under the constant relaxation time approximation [25]. A dense mesh of 130000 k points was used to obtain accurate transport properties.

## 3. Results and discussions

### 3.1. Structural properties

The double perovskite $Sr_2TiCoO_6$ crystallizes in an ideal cubic structure as shown in Fig. 1, with space group $Fm\bar{3}m$ (225) according to Hermann-Maguin convention, where Sr atoms occupy 8c (0.25, 0.25, 0.25), Ti at 4b (0.5, 0.5, 0.5) sites, Co on 4a (0, 0, 0) and O at 24e (0.25, 0, 0) of cubic unit cell [26]. The experimental lattice parameters have been optimized using Birch-Murnaghan's [27] equation of state by fitting energy versus cell volume in nonmagnetic (NM) and ferromagnetic (FM) cases. From Fig. 2 it is clearly shown that the lowest energy corresponds to the ferromagnetic phase with an optimized lattice parameter of 7.76 Å. The calculated ground state parameters which include bulk modulus ($B_0$), lattice constant (A), and pressure derivative of bulk modulus are displayed in Table I. It is clear that the calculated lattice constant of $Sr_2TiCoO_6$ mentioned in Table I is close to the

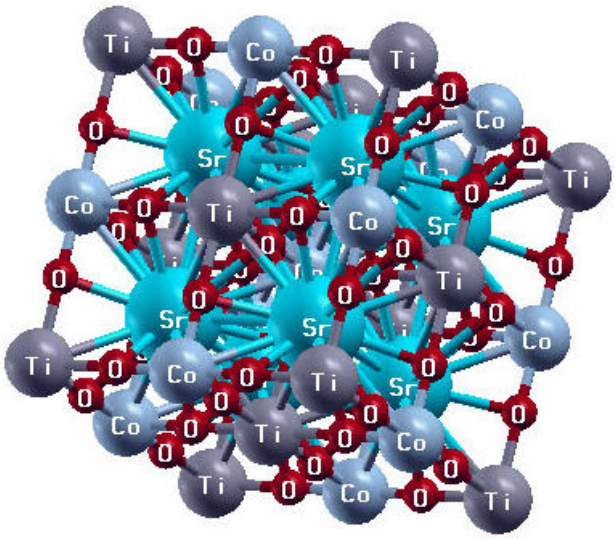


FIGURE 1. Crystal structure of double perovskite $Sr_2TiCoO_6$.

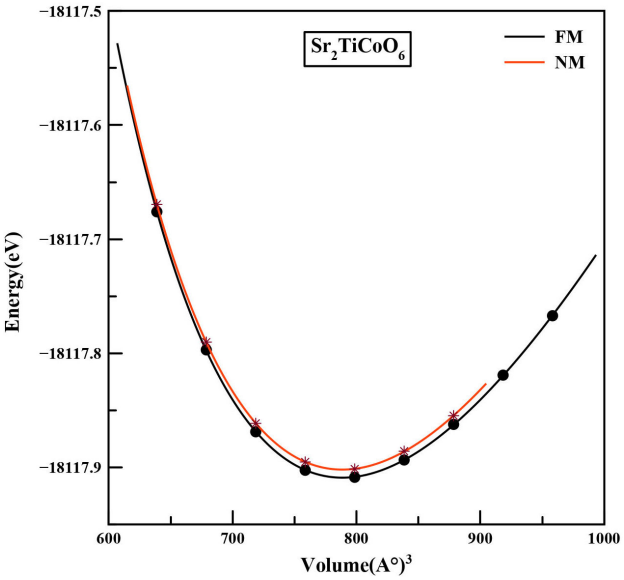


FIGURE 2. Structural optimization plots of $Sr_2TiCoO_6$ in ferromagnetic (FM) and non-magnetic (NM) phases.

TABLE I. Calculated values of lattice constant a(Å), unit cell volume, bulk modulus B (GPa), pressure derivative of bulk modulus B' and ground-state energies $E_0$ (Ry) of $Sr_2TiCoO_6$ double perovskite.

| | Present work | Other |
|---|---|---|
| Method | GGA | Exp |
| a(Å) | 7.76 | 7.35 [18] |
| V (Å$^3$) | 788.3819 | - |
| B (GPa) | 164.0811v | - |
| B' | 4.55 | - |
| $E_0$: Minimum total energy per unit cell (Ry) | -18117.909431 | - |

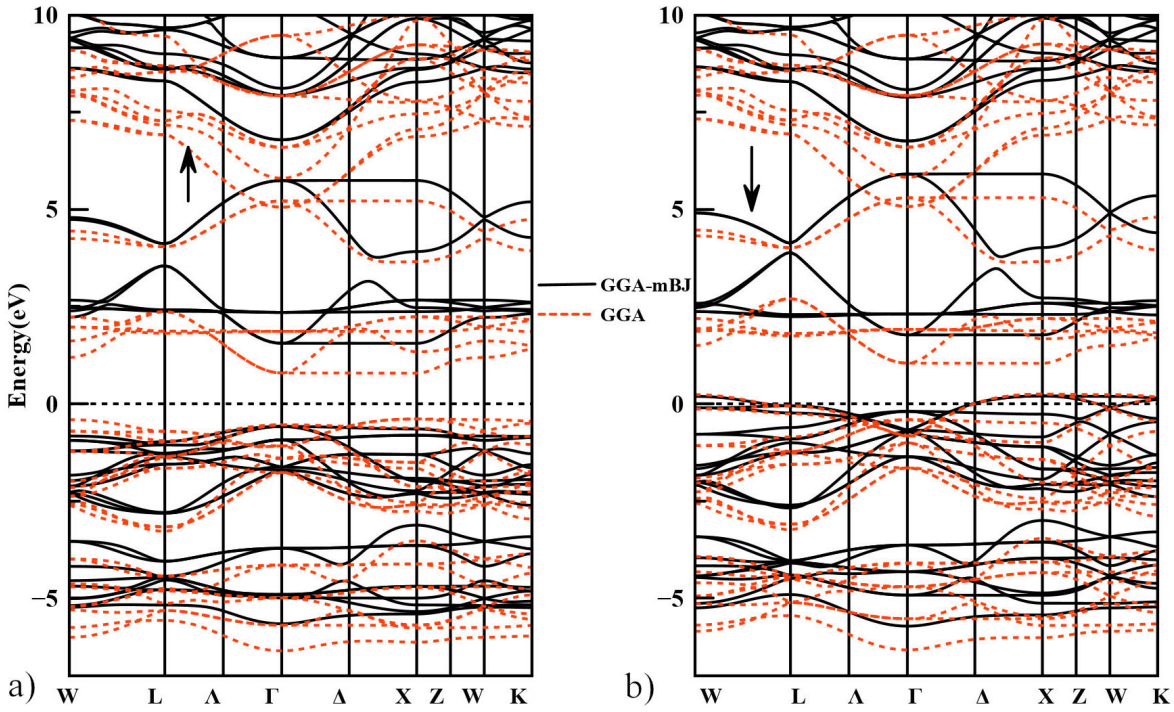


FIGURE 3. The band structures of $Sr_2TiCoO_6$ for both spin channels with GGA and mBJ approaches.

available experimental data [18]. Also, the deviation of calculated oxygen parameter $x$ from the ideal value of 0.25 is assumed in the simple perovskite structure. Since there is no available experimental or theoretical data to compare the bulk modulus and its derivative, our results are predictive and can help potential investigations.

The stability of the material was also checked by calculating the tolerance factor ($\tau$) as:

$$\tau = 0.707 \frac{s_{Sr} + r_0}{\left(\frac{r_{Co}+r_{Ti}}{2}\right) + r_0} \quad (1)$$

Where $r_{Sr}$ is the ionic radius of the Strontium atom, $r_0$ is the ionic radius of the oxygen atom, $r_{Ti}$ is the ionic radius of the Titane atom, and $r_{Co}$ is the ionic radius of the Cobalt atom. Materials with $\tau$ in the range of 0.9 to 1.0 have a perfect cubic structure, and $\tau$ greater than 1.0 results in a hexagonal structure [28]. The value of the tolerance factor computed for $Sr_2TiCoO_6$ is equal to 0.92.

### 3.2. Electronic and magnetic properties

The spin-polarized electronic band structures of $Sr_2TiCoO_6$ along the high-symmetry Brillouin zone points have been studied using GGA and mBJ approximations, as presented in Fig. 3. In order to have the correct estimation of the band-gap in spin up channels which is usually underestimated by GGA, mBJ has been used. First, in the case of the spin-up channel, we can distinguish the Fermi level in the middle of the band-gap showing the semiconducting nature. While for spin-down states it is clear that the fermi level is completely occupied, presenting the metallic nature in both approximation methods. As seen from the band profiles using both approximated schemes, half-metallicity is achieved, and the studied material can find various applications in spin-based devices. The value of the gap using GGA is different from the one using mBJ, and it is equal to 1.18 eV, 2.14 eV, respectively, at symmetric points '$X$' and 'Γ', generating an indirect band-gap. The gap increases as we go from GGA to mBJ.

The mechanism of magnetism in the double perovskite (DP) compound has been extensively discussed [29,30,31,32]. In the crystal structure shown in Fig. 1, the magnetism in the material can be understood in terms of an ionic description where the Co5+ ($3d^3$) and the Ti4+ ($3d^2$) ions occupy alternating ionic positions along the three axes of the larger cube with consecutive anti-parallel spin alignment, suggesting a total magnetic moment of 1 $\mu$B per formula unit (f.u.) for the system. However, the half-metallic states and consequently the magnetic moments are critically dependent on the perfect ordering of the Co and Ti sites. In order to unravel the origin of the magnetism in the Sr2TiCoO6 series, we have first investigated the electronic density of states (DOS) of this compound. Figure 4 shows the DOS as obtained in spin-polarized DFT calculations within GGA-mBJ method. The peaks below -6.2 eV to about -4.5 eV are a mix between the Co-eg d and Co-t2g d states. While the peaks below -1.2 eV refer mostly to oxygen contributions. The peaks crossing the Fermi level and ranging from -1.2 eV to about 0.3 eV belong mainly to Co-t2g d states and some slight admixture of oxygen p states. The presence of approximate

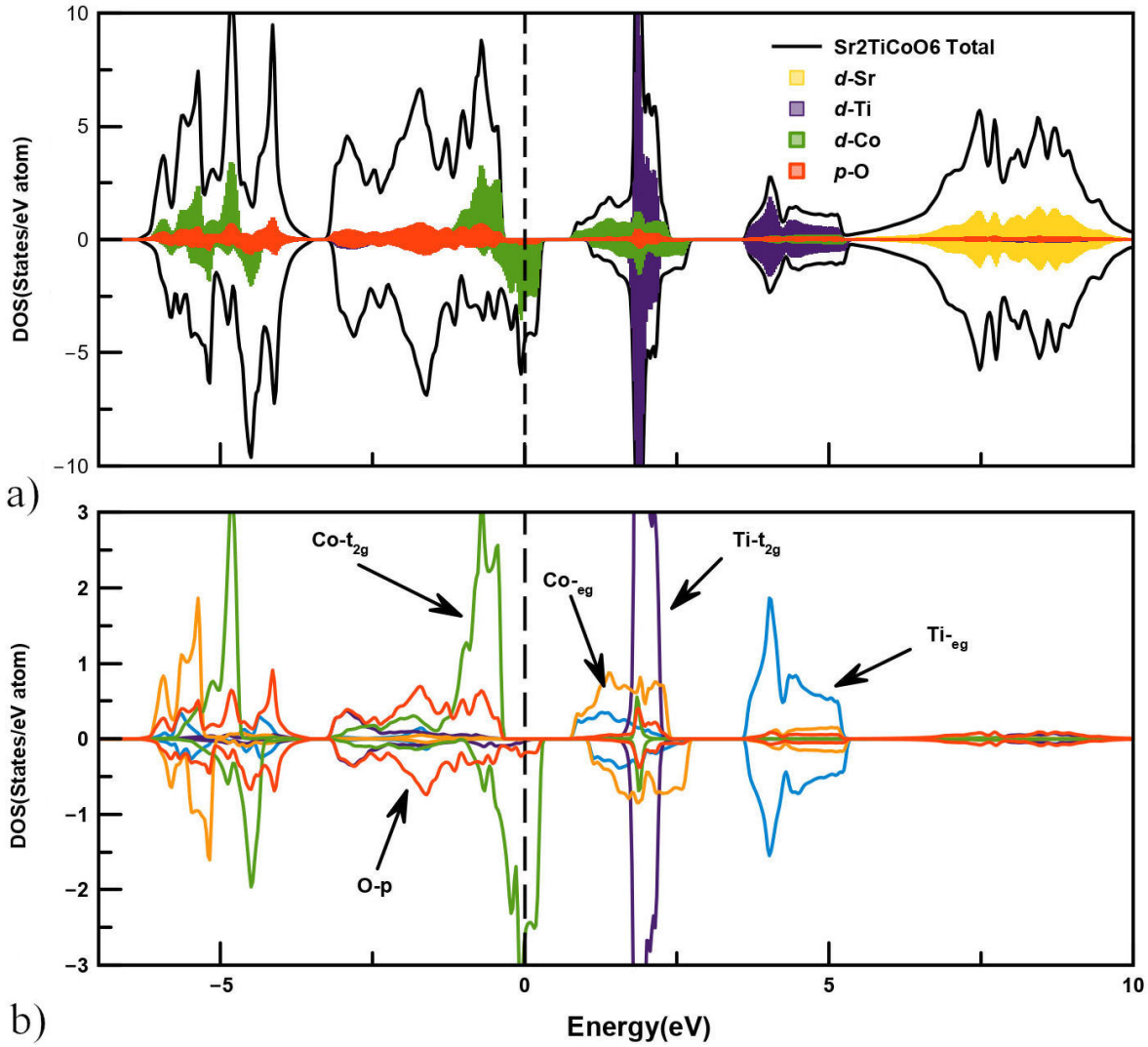


FIGURE 4. Combined total and partial density of states for $Sr_2TiCoO_6$ using GGA-mBJ approaches.

TABLE II. Calculated partial, Interstitial and total magnetic moment and band gap (eV) for $Sr_2TiCoO_6$ within GGA and mBJ (in Bohr magneton $\mu$B).

| Compound | Method | Magnetic Moment ($\mu$B) | | | | | | Band Gap (eV) |
|---|---|---|---|---|---|---|---|---|
| | | Interstial | Sr | Ti | Co | O | Total | |
| $Sr_2TiCoO_6$ | GGA | 0.0523 | 0.0029 | -0.0708 | 0.718 | 0.0486 | 0.9972 | 1.18 |
| | mBJ | -0.0394 | -0.0026 | -0.0989 | 0.6662 | 0.0796 | 1 | 2.14 |

cubic symmetry of the octahedral coordination of oxygen atoms around the transition metal sites results in a splitting of the d levels into d-t2g and d-eg orbitals. The Co-t2g peaks are partially filled in the minority spin channel, while the Co-eg, Ti-t2g, and Ti-eg bands remain empty.

The occupied part of the bands near the Fermi level in the majority spin channel [see Fig. 4] is mainly composed of Co d states, which hybridize with the oxygen p states. The narrow bands lying directly above the Fermi level covering an energy range of about 0.8 to 2.2 eV are mostly from Co-eg and Ti-t2g contributions, while the Ti-eg bands are high in energy.

Furthermore, the calculated individual, interstitial, and total magnetic moments have also been calculated with GGA and mBJ. Our compound has a ferromagnetic nature with a total magnetic moment of nearly 1 $\mu$B which is the summation of the partial moments from various atoms and the interstitial sites. Sr, Ti, and O atoms show a very small contribution to the total magnetic moment, which is almost negligible as displayed in Table II. The main contributions to the total

magnetic moment come from the Co atom, where its partial moment is of 0.718 $\mu$B (GGA) and 0.6662 $\mu$B (mBJ). The FM nature for $Sr_2TiCoO_6$ is predominately due to cobalt atoms. The main source of magnetization in this compound is from unfilled Co-3d orbitals. The positive value of the magnetic spin moment is due to cobalt, whereas the low negative value is attributed to Titane. Comparing to other experimental reported results it is shown that antiferromagnetic-type coupling dominates over weak ferromagnetic coupling in the STC system [33].

### 3.3. Elastic and mechanical properties

Elastic properties not only provide a decent and dynamic suggestion of the system but also give us better knowledge of the material strength for its technological applications. These constants give concrete and necessary comprehension of solid mechanical stability under different forces.

In this study, we investigated the mechanical and elastic properties of $Sr_2TiCoO_6$. The elastic constants were obtained by calculating energy about the tetragonal and rhombohedral strain [34]. Only three independent elastic constants ($C_{11}$, $C_{12}$, and $C_{44}$) are used for materials with cubic symmetry. The values of these elastic constants under ambient conditions were determined and shown in Table III. For cubic structures under ambient condition the stability criteria is: ($C_{11}$ - $C_{12}$) $> 0$, $C_{11} > 0$, $C_{44} > 0$, ($C_{11}$+2$C_{12}$) $> 0$, $C_{12} <$ B $< C_{11}$, where $C_{11}$ stands the compressive resistance along the direction of $X$-axis. Also, the value of $C_{11}$ indicates a larger value as compared to other values, which suggests the incompressible essence of the material, $C_{12}$ indicates transverse strain, $C_{44}$ is shear modulus and B represents bulks modulus. The calculated values of elastic constants strictly follow the generalized mechanical stability criteria [35].

Additionally, these elastic parameters are related to other mechanical properties through empirical expressions displayed as [36].

$$E = \frac{9BG}{3B+G},$$
$$B = \frac{C_{11}+2C_{12}}{3},$$
$$\nu = \frac{3B-2G}{2(2B+G)}$$
$$A = \frac{2C_{44}}{C_{11}-C_{12}}.$$

Where $E$ and $B$ are Young's and Bulk's moduli respectively. $\nu$ is a Poisson's ratio and $A$ is an anisotropy ratio which are listed in Table III. Bulk modulus describes the stiffness of a material, the higher the value of $B$, the higher its stiffness resistance is. The calculated value of bulk modulus of $Sr_2TiCoO_6$ is largely showing strong resistance to volumetric change caused by applied stress. The shear modulus ($G$), which characterizes the calculated plastic twist of material, has been obtained from the Voigt-Reuss-Hill approximation [37,38] using the arithmetic mean of Voigt, $G_V$, and Reuss $G_R$, presented in Table III and calculated as:

$$G_V = \frac{C_{11}-C_{12}-3C_{44}}{5} = 137.08,$$
$$G_R = \frac{5C_{44}(C_{11}-C_{12})}{(4C_{44}+3[C_{11}-C_{12}])} = 135.85,$$
$$G = \frac{1}{2}(G_V+G_R) = 136.46.$$

The value of Young's modulus ($E$) was obtained from the bulk modulus ($B$) and the shear modulus ($G$) [8]. As ($E$) defines the strength of the material, the higher the value of ($E$), the higher its strength is. The obtained value of ($E$) was calculated to be 334.05 GPa, which is large enough, and therefore $Sr_2TiCoO_6$ acts as a hard material.

Poisson's ratio '$\nu$' is used to evaluate the ductility and brittleness of a compound. The material has a ductile nature if its value is greater than 0.26; otherwise, the material is considered to be brittle. Table II shows that Poisson's ratio for $Sr_2TiCoO_6$ was found to be lower than 0.26, which confirms its brittle nature. Poisson's ratio '$\nu$' also gives knowledge about the estimation of bonding nature [39,40] in a material. According to this limit, the type of material bonding will be ionic if $\approx 0.25$, covalent if $\approx 0.10$, and metallic if $\approx 0.33$. For our compound, $\nu$ is found close to 0.25 and thus major bonding in these materials is ionic.

The Pugh's ratio [41] is another stability criterion to define whether the material is ductile or brittle. Its numerical or index value is $1.75.B/G > 1.75$ indicates the ductile na-

TABLE III. Elastic constants $C_{11}$, $C_{12}$, $C_{44}$ in (GPa), Bulk modulus $B$ (GPa), Shear Modulus $G$ (GPa), Young's modulus $E$ (GPa), Poisson's ratio $\nu$, Zener anisotropy factor A. Pugh's ratio ($B/G$), Cauchy's pressure ($C_{12}$-$C_{44}$), and melting temperature Tm (K) for $Sr_2TiCoO_6$.

| Mechanical Properties and Melting Temperature | Alloy $Sr_2TiCoO_6$ |
|---|---|
| $C_{11}$ | 402.1 |
| $C_{12}$ | 95.6 |
| $C_{44}$ | 126.3 |
| $B$ | 197.77 |
| $G_V$ | 137.08 |
| $G_R$ | 135.85 |
| $G$ | 136.46 |
| $E$ | 334.05 |
| $\nu$ | 0.22 |
| $B/G$ | 1.44 |
| $C_{12}$-$C_{44}$ | -30 |
| $A$ | 0.82 |
| $T_m$ | 2929.81 |

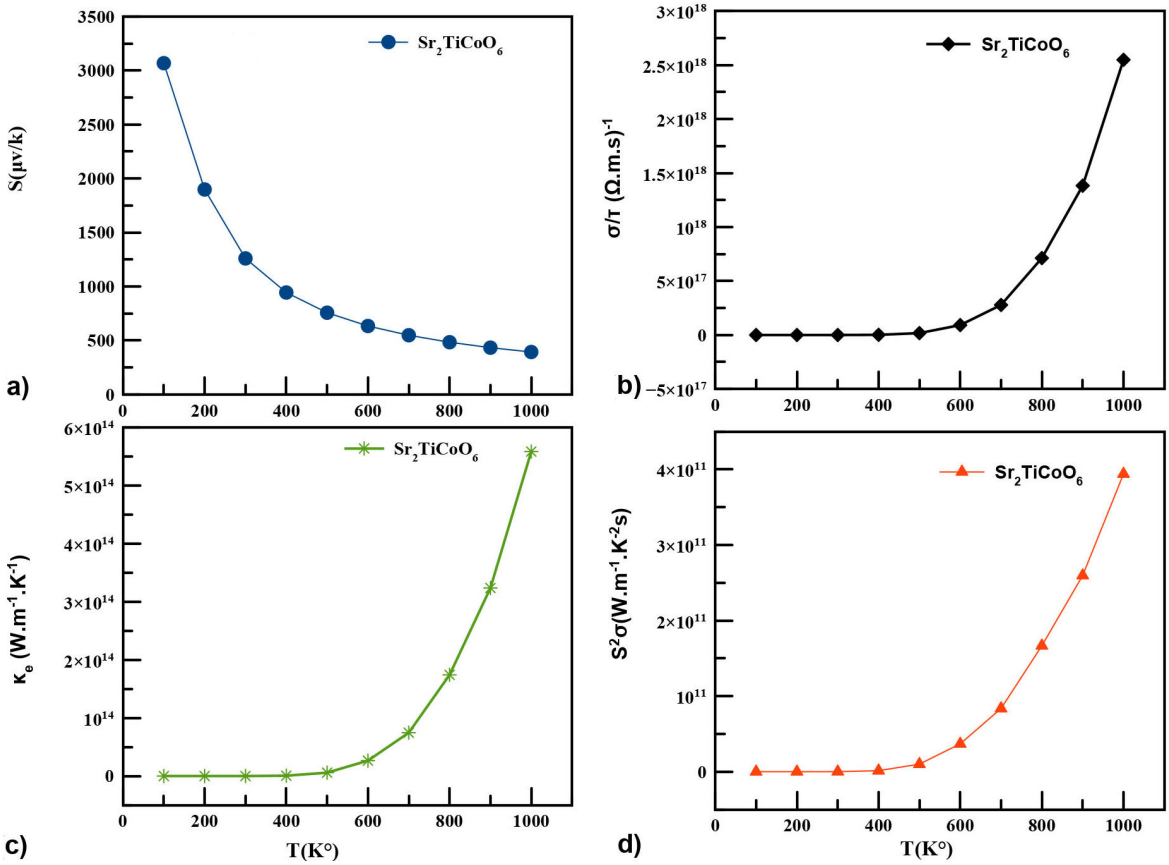


FIGURE 5. a) Variation of electrical conductivity ($\sigma/\tau$), b) Seebeck coefficient ($S$), c) electronic thermal conductivity ($S$), d) power factor (PF) as a function of temperature for the $Sr_2TiCoO_6$ compound.

ture while the value of $B/G < 1.75$ is associated with the brittle character of the material. From the observed data, the computed value of $B/G$ for $Sr_2TiCoO_6$ compound is $< 1.75$. Consequently, it has a brittle nature.

The brittle nature was also verified from Cauchy's pressure relation [42] defined as ($C_{12}$-$C_{44}$). A positive value indicates that the material is ductile otherwise the nature is identified as brittle. For $Sr_2TiCoO_6$ it is clear that Cauchy's pressure is negative which emphasizes its brittle nature.

Zener's anisotropy factor (A) describes the degree of the elastic anisotropy of the solid. For an isotropic material, the anisotropy factor (A) is equal to one, while any different value shows anisotropy [43]. From Table III, it was found to be 0.82 (less than 1), signifying that the material has elastic anisotropic nature.

There are no theoretical or experimental data on the elastic properties of this compound for which we can compare our work. We believe that in the future, our work can encourage further research in this direction.

The melting temperature is also a further thermodynamic quantity which has been calculated using the following empiric expression [44] as described below.

$$T_m(K) = [553\ (\mathrm{K}) + (5.911)C_{11}]\ \mathrm{GPa}\ \pm 300\ \mathrm{K}$$

The corresponding observed value for the present alloy is $2929.81 \pm 300$ K and thus suggests that the material has a strong capability to maintain its crystal structure over a large range of temperatures.

### 3.4. Thermoelectric properties

Thermoelectric materials (TE) have the potential to convert waste heat into usable energy [45]. Because of their energy convergence management, these materials are currently being studied at faster levels rather than other technologically appropriate materials.

To explore the electronic transport properties of $Sr_2TiCoO_6$ layered perovskite, we have made use of semi-classical Boltzmann theory as employed in BoltzTraP code [25]. In order to have potential thermoelectric properties in a material, it needs to have a large value of electrical conductivity ($\sigma/\tau$), a large value of Seebeck coefficient ($S$), and very low electronic thermal conductivity ($\kappa e/\tau$).

In this article, the thermoelectric parameters in the range of temperatures from 100 K to 1000 K have been reported, in Fig. 5(a). The electrical conductivity per relaxation time ($\sigma/\tau$) as a function of temperature for $Sr_2TiCoO_6$ is represented, we can observe that electrical conductivity increases with increasing temperature until reaching a maximum value

of $2.5488 \times 10^{18}$ $(\Omega ms)^{-1}$ at 1000 K. Electrical conductivity is about $19.189 \times 10^3$ at low temperatures (100 K). The variation of the Seebeck coefficient ($S$) as a function of temperature is shown in Fig. 5b). It is clearly apparent from the plot that the Seebeck coefficient ($S$) decreases to a minimum of 393.15 $\mu$V/K with an increase in temperature. The Seebeck coefficient is positive, meaning $p-$type conduction. At 100 K, a maximum value of 3068.24 $\mu$V/K was obtained. Figure 5c) depicts the response of electronic thermal conductivity ($\kappa e/\tau$) within 100 K and 1000 K for $Sr_2TiCoO_6$. The figure clearly shows that the nature of ($\kappa e/\tau$) is increasing with increasing temperature. The value of ($\kappa e/\tau$) increases from 18.09 W/mKs at 100 K to $5.58 \times 10^{14}$ W/mKs at 1000 K. In order to estimate the thermoelectric efficiency of $Sr_2TiCoO_6$, we calculated the fluctuation of the power factor over a large temperature range as shown in Fig. 5d). We can observe that PF increases slightly with rising temperatures, from $1.806 \times 10^{11}$ (W.m$^{-1}$.K$^{-2}$s) at 100 K until reaching the value of $3.939 \times 10^{11}$ (W.m$^{-1}$.K$^{-2}$s) at 1000 k. The thermoelectric values found for $Sr_2TiCoO_6$ are definitely higher to those reported experimentally for $Ba_xSr_{2-x}TiCoO_6$ with $x = 0.0$, $x = 0.10$, $x = 0.15$, and (d) $x = 0.2$ [46]. The obtained results from the first principles calculation reveal that $Sr_2TiCoO_6$ is a promising thermoelectric material.

## 4. Conclusion

The first-principles calculations have been performed to predict the structural parameters, elastic, magneto-electronic, and transport properties of $Sr_2TiCoO_6$ double perovskite. GGA and TB-mBJ potential were used for exchange-correlation. $Sr_2TiCoO_6$ is stable in a cubic structure with a lattice constant of 7.76 Å. The lattice constant from our calculations is found to agree well with the experimental data. The calculated elastic constants have been found to follow the mechanical stability criteria. Cauchy pressure, Pugh's and Poisson's ratio altogether confirm that $Sr_2TiCoO_6$ is brittle in nature. Also, the material was determined to have a high melting temperature value equal to $2929.81 \pm 300$ K. The electronic results display an indirect half-metallic nature, semiconducting in spin-up channels and metallic in spin-down channels.

Total and individual magnetic moments indicate that the Co atom is responsible for ferromagnetism. Transport coefficients such as Seebeck coefficient, electrical conductivity, thermal conductivity, and power factor have been measured by using BoltzTraP. The envisaged overall properties validate that this alloy is a promising candidate for applications in thermoelectric and spintronic applications.

## Acknowledgments

The research was supported by the General Division for Algerian scientific Research and technological development (DG-RSDT). https://www.mesrs.dz/dgrsdt.

1. G. S. Alemán-Nava, *et al.*, Renewable energy research progress in Mexico: *A review. Renew. Sust. Energ. Rev.*, **32** (2014) 140. doi:10.1016/j.rser.2014.01.004
2. P. W. Barnes, *Exploring Structural Changes and Distortions in Quaternary Perovskites and Defectpyrochlores Using Powder Diffraction Techniques*, (The Ohio State University, Ohio, Columbus, 2003).
3. G. Pilania, *et al.* Machine learning bandgaps of double perovskites. *Sci. Rep.* **6** (2016) 19375. https://doi.org/10.1038/srep19375
4. P. Villar Arribi, P. García-Fernández, J. Junquera, and V. Pardo, Efficient thermoelectric materials using nonmagnetic double perovskites with $d^0/d^6$ band filling. *Phys. Rev. B*, **94** (2016). doi:10.1103/physrevb.94.035124
5. S. Ghosh, and D. C. Gupta, Electronic, magnetic, elastic and thermodynamic properties of $Cu_2MnGa$. *J. Magn. Magn. Mater*. **411** (2016) 120. https://doi.org/10.1016/j.jmmm.2016.03.044
6. S. Ohta, T. Nomura, H. Ohta, and K. Koumoto, High-temperature carrier transport and thermoelectric properties of heavily La- or Nb-doped $SrTiO_3$ single crystals. *J. Appl. Phys*. **97** (2005) 034106. doi:10.1063/1.1847723
7. M. Liu, M. B. Johnston, and H. J. Snaith, Efficient planar heterojunction perovskite solar cells by vapour deposition. *Nature,* **501** (2013) 395. doi:10.1038/nature12509
8. S. A. Dar, V. Srivastava, and U. K. Sakalle, Ab Initio High Pressure and Temperature Investigation on Cubic $PbMoO_3$ Perovskite. *J. Electron. Mater.*, **46** (2017) 6870. doi:10.1007/s11664-017-5731-2
9. Z. Ali, I. Ahmad, I. Khan, and B. Amin, Electronic structure of cubic perovskite $SnTaO_3$. Intermetallics, **31** (2012) 287. doi:10.1016/j.intermet.2012.08.001
10. Y. Shi, *et al.*, High-Pressure Synthesis of 5d Cubic Perovskite $BaOsO_3$ at 17 GPa: Ferromagnetic Evolution over 3d to 5d Series. *J. Am. Chem. Soc.* **135** (2013) 16507. doi:10.1021/ja4074408
11. Z. Ali, A. Sattar, S. J. Asadabadi, and I. Ahmad, Theoretical studies of the osmium based perovskites $AOsO_3$ (A=Ca, Sr and Ba). *J. Phys. Chem. Solids* **86** (2015) 114. doi:10.1016/j.jpcs.2015.07.001
12. R. Chaurasiya, S. Auluck, and A. Dixit, Cation modified A 2 (Ba, Sr and Ca) ZnWO 6 cubic double perovskites: *A theoretical study. Comput. Condens. Matter* **14** (2018) 27. doi:10.1016/j.cocom.2017.12.005
13. T. M. Bhat, and D. C. Gupta, Robust thermoelectric performance and high spin polarisation in CoMnTiAl and FeMnTiAl

compounds. *RSC Advances* **6** (2016) 80302. doi:10.1039/c6ra18934b

14. Y. Takahashi, H. Hasegawa, Y. Takahashi, and T. Inabe, Hall mobility in tin iodide perovskite $CH_3NH_3SnI_3$: Evidence for a doped semiconductor. *J. Solid State Chem*. **205** (2013) 39. doi:10.1016/j.jssc.2013.07.008
15. Y. He, and G. Galli, Perovskites for Solar Thermoelectric Applications: A First Principle Study of $CH_3NH_3AI_3$ (A = Pb and Sn). *Chem. Mater*. **26** (2014) 5394. doi:10.1021/cm5026766
16. M. Acharya, and T. Maiti, Effect of bismuth doping on thermoelectric properties of $Sr_2$ $TiCoO_6$. *Ferroelectrics*, **532** (2018) 28. doi:10.1080/00150193.2018.1430432
17. M. Saxena, and T. Maiti, Compositional modification of $Sr_2TiCoO_6$ double perovskites by Mo and La for high temperature thermoelectric applications. *Ceram. Int.*, **44** (2018) 2732. doi:10.1016/j.ceramint.2017.11.003
18. Sudha, M. Saxena, K. Balani, and T. Maiti, Structure and thermoelectric properties of calcium doped $sr_2ticoo_6$ double perovskites. *Mat. Sci. Eng. B*, **244** (2019) 65. doi:10.1016/j.mseb.2019.04.025
19. E. Wimmer, H. Krakauer, M. Weinert, and A. J. Freeman, Full-potential self-consistent linearized-augmented-plane-wave method for calculating the electronic structure of molecules and surfaces: O2 molecule. *Phys. Rev. B*, **24** (1981) 864. doi:10.1103/physrevb.24.864
20. P. Blaha, K. Schwartz, G.K.H. Madsen, D. Kvasnicka and J. Liutz, *WIEN2k An Augmented Plane Wave Plus Local OrbitalsProgram for calculating Cristal Properties* (Vienna University of Technology, Vienna, Austria, 2001).
21. J. P. Perdew, K. Burke, and M. Ernzerhof, Generalized Gradient Approximation Made Simple. *Phys. Rev. Lett.*, **77** (1996) 3865. doi:10.1103/physrevlett.77.3865
22. A. D. Becke, and E. R. A Johnson, simple effective potential for exchange. *Int. J. Chem. Phys*., **124** (2006) 221101. doi:10.1063/1.2213970
23. S. A. Sofi, S. Yousuf, and D. C. Gupta, Prediction of robustness of electronic, magnetic and thermoelectric properties under pressure and temperature variation in Co2MnAs alloy. *Comput. Condens. Matter*, e00375 (2019). doi:10.1016/j.cocom.2019.e00375
24. T. Charpin, A Package for Calculating elastic tensors of cubic phases using WIEN: Laboratory of Geometrix F-75252 (Paris, France) (2001).
25. G. K. H. Madsen, and D. J. Singh, BoltzTraP. A code for calculating band-structure dependent quantities. *Comput. Phys. Commun.*, **175** (2006) 67. doi:10.1016/j.cpc.2006.03.007
26. S. A. Khandy and D. C. Gupta, Magneto-electronic, Mechanical, Thermoelectric and Thermodynamic Properties of Ductile Perovskite $Ba_2SmNbO_6$. *Mater. Chem. Phys*., **121983** (2019). doi:10.1016/j.matchemphys.2019.121983
27. F. Birch, The Effect of Pressure Upon the Elastic Parameters of Isotropic Solids, According to Murnaghan's Theory of Finite Strain. *J. Appl. Phys*, **9** (1938) 279. doi:10.1063/1.1710417
28. Z. Li, M. Yang, J.-S. Park, S.-H. Wei, J. J. Berry, and K. Zhu, Stabilizing Perovskite Structures by Tuning Tolerance Factor: *Formation of Formamidinium and Cesium Lead Iodide Solid-State Alloys. Chem. Mater*., **28** (2015) 284. doi:10.1021/acs.chemmater.5b04107
29. T. Saha-Dasgupta, Magnetism in Double Perovskites. *J Supercond Nov Magn* **26** (2013) 1991. https://doi.org/10.1007/s10948-012-1920-7
30. H. Das, P. Sanyal, T. Saha-Dasgupta, and D. D. Sarma, Origin of magnetism and trend inTcin Cr-based double perovskites: Interplay of two driving mechanisms. *Phys. Rev. B*, **83** (2011). doi:10.1103/physrevb.83.104418
31. D. D. Sarma, P. Mahadevan, T. Saha-Dasgupta, S. Ray, and A. Kumar, Electronic Structure of$Sr_2FeMoO_6$. *Phys. Rev. Let*., **85** (2000) 2549. doi:10.1103/physrevlett.85.2549
32. Saha-Dasgupta, T. Double perovskites with 3d and 4d/5d transition metals: compounds with promises. *Mater. Res. Express*, **7** (2020) 014003. doi:10.1088/2053-1591/ab6293
33. D. Sri Gyan *et al.* Magnetic and Electron Spin Resonance Properties of $Ba_xSr_{2-x}TiCoO_6$ Double Perovskites. *Phys. Stat. Sol. (b) 257* (2020) 1. doi:10.1002/pssb.201900341
34. M. J. Mehl, J. E. Osburn, D. A. Papaconstantopoulos, and B. M. Klein, Structural properties of ordered high-melting-temperature intermetallic alloys from first-principles total-energy calculations. *Phy. Rev. B*, **41** (1990) 10311. doi:10.1103/physrevb.41.10311
35. G. V. Sinko, and N. A. Smirnov, Ab initio calculations of elastic constants and thermodynamic properties of bcc, fcc, and hcp Al crystals under pressure. *J. Phys: Condens. Matter.* **14** (2002) 6989. doi:10.1088/0953-8984/14/29/301
36. F. Birch, The Effect of Pressure Upon the Elastic Parameters of Isotropic Solids, According to Murnaghan's Theory of Finite Strain. *J. Appl. Phys*, **9** (1938) 279. doi:10.1063/1.1710417
37. R. Hill, The Elastic Behaviour of a Crystalline Aggregate. *Proc. Phy. Soc. Lon. Section A*, **65** (1952) 349. doi:10.1088/0370-1298/65/5/307
38. A. Reuss, Berechnung der Flie$\beta$grenze von Mischkristallen auf Grund der Plastizitätsbedingung für Einkristalle. *ZAMM-Zeitschrift Für Angewandte Mathematik Und Mechanik*, **9** (1929) 49. doi:10.1002/zamm.19290090104
39. D. G. Pettifor, Theoretical predictions of structure and related properties of intermetallics. *Mater. Sci. Technol*, **8** (1992) 345. doi:10.1179/mst.1992.8.4.345
40. J. Haines, J. Léger, and G. Bocquillon, Synthesis and Design of Superhard Materials. *Annual Rev. Mater. Sci.* , **31** (2001) 1. doi:10.1146/annurev.matsci.31.1.1
41. S.F. Pugh, *Philos. Mag*. **45** (1954) 823. https://doi.org/10.1080/14786440808520496
42. M. Nabi, T. M. Bhat, and D. C. Gupta, Magneto-Electronic, Thermodynamic, and Thermoelectric Properties of 5f-Electron System $BaBkO_3$ *J. Supercond. Nov. Magnetism* **32** (2018) 1751. doi:10.1007/s10948-018-4872-8
43. B.benichou, Z.Nabi, B.Bouabdallah, H.Bouchenafa. Ab initio investigation of the electronic structure, elastic and magnetic properties of quaternary Heusler alloy $Cu_2MnSn_{1-x}In_x$ ($x = 0$, 0.25, 0.5, 0.75, 1). *Rev Mex Fis* **64**, (2018) 135. https://doi.org/10.31349/RevMexFis.64.135

44. M. E. Fine, L. D. Brown, and H. L. Marcus, Elastic constants versus melting temperature in metals. *Scr. Mettal*, **18** (1984) 951. doi:10.1016/0036-9748(84)90267-9

45. S. A. Khandy, and D. C. Gupta, Electronic structure, magnetism and thermoelectricity in layered perovskites: $Sr_2SnMnO_6$ and $Sr_2SnFeO_6$. *J. Magn. Magn. Mater*, **441** (2017) 166. doi:10.1016/j.jmmm.2017.05.058

46. M. Saxena, P. Roy, M. Acharya, I. Bose, K. Tanwar, and T. Maiti, Enhanced thermoelectric figure-of-merit in environmentally benign BaxSr2-xTiCoO6 double perovskites. *Appl. Phy. Let.*, **109** (2016) 263903. doi:10.1063/1.4973281